Global Nonradial Instabilities of Dynamically Collapsing Gas Spheres

Dong Lai [1]

Center for Radiophysics and Space Research, Department of Astronomy, Cornell University, Ithaca, NY 14853

ABSTRACT

Self-similar solutions provide good descriptions for the gravitational collapse of spherical clouds or stars when the gas obeys a polytropic equation of state, $p = K\rho^\gamma$ (with $\gamma \leq 4/3$, and $\gamma = 1$ corresponds to isothermal gas). We study the behaviors of nonradial (nonspherical) perturbations in the similarity solutions of Larson, Penston and Yahil, which describe the evolution of the collapsing cloud prior to core formation. Our global stability analysis reveals the existence of unstable bar-modes ($l = 2$) when $\gamma \leq 1.09$. In particular, for the collapse of isothermal spheres, which applies to the early stages of star formation, the $l = 2$ density perturbation relative to the background, $\delta\rho(\mathbf{r}, t)/\rho(r, t)$, increases as $(t_0 - t)^{-0.352} \propto \rho_c(t)^{0.176}$, where t_0 denotes the epoch of core formation, and $\rho_c(t)$ is the cloud central density. Thus, the isothermal cloud tends to evolve into an ellipsoidal shape (prolate bar or oblate disk, depending on initial conditions) as the collapse proceeds. This shape deformation may facilitate fragmentation of the cloud. In the context of Type II supernovae, core collapse is described by the $\gamma \simeq 1.3$ equation of state, and our analysis indicates that there is no growing mode (with density perturbation) in the collapsing core before the proto-neutron star forms, although nonradial perturbations can grow during the subsequent accretion of the outer core and envelope onto the neutron star.

We also carry out a global stability analysis for the self-similar expansion-wave solution found by Shu, which describes the post-collapse accretion ("inside-out" collapse) of isothermal gas onto a protostar. We show that this solution is unstable to perturbations of all l's, although the growth rates are unknown.

Subject headings: hydrodynamics — instabilities — stars: formation – supernovae — ISM: clouds

1. Introduction

The gravitational collapse of molecular clouds leading to star formation has long been an active area of study. In the early stages of collapse (from $\rho \lesssim 10^{-19}$ g cm^{-3} to $\rho \sim 10^{-12}$ g cm^{-3}) the gas

---

[1]E-mail: dong@spacenet.tn.cornell.edu; Alfred P. Sloan Research Fellow

remains approximately isothermal (at temperature ~ 10 K) due to efficient cooling by dust grains (see, e.g., Myhill & Boss 1993). The gas dynamics is then specified by two dimensional parameters, the gravitational constant G and the isothermal sound speed a, so that the flow is expected to approach a self-similar form in the asymptotic limit, when the memory of initial conditions is "lost". Larson (1969) and Penston (1969) found a similarity solution which describes the pre-collapse (i.e., before the central protostar forms) evolution of the cloud, in which the gas collapses from rest, accelerating until it cruises at Mach number of 3.3 and the density profile reaches a r^{-2} power law. The Larson-Penston solution contains a nonsingular homologous inner core and a supersonic outer envelope. A qualitatively different set of similarity solutions was found by Shu (1977). Of particular interest is Shu's expansion-wave solution which describes the post-collapse accretion of a singular isothermal gas cloud onto a protostar. In this solution, the flow starts from hydrostatic equilibrium (with a r^{-2} density profile) and a rarefaction wave expands from the center and initiates the collapse (the so-called "inside-out" collapse); Inside the expansion-wave front, the flow eventually attains the free-fall behavior ($v \propto r^{-1/2}$) at small radii, with density $\rho \propto r^{-3/2}$. The link between the Larson-Penston pre-collapse solution and Shu's expansion-wave solution was elucidated by Hunter (1977), who showed that the Larson-Penston solution can be continued to the post-collapse phase and that there exists an infinite (but discrete) number of pre- and post-collapse solutions of a different type (called "Type I"; see §2), among which the expansion-wave solution represents a limiting case. Figure 1 illustrates the properties of different self-similar solutions for the collapse and accretion of isothermal spheres.[2]

With the plethora of possible similarity solutions, it is important to know which, if any, of them are actually realized by collapse of isothermal clouds. One-dimensional hydrodynamical simulations, starting from a regular (Bonner-Ebert) sphere, generally indicate that the collapse resembles the Larson-Penston similarity form in the asymptotic limit (Hunter 1977; Foster & Chevalier 1993). This is consistent with the recent finding of Hanawa & Nakayama (1997), who showed that the pre-collapse Type I solutions of Hunter's (see Fig. 1) are strongly unstable against global spherical perturbations, and therefore are unlikely to be realized in astrophysical situations or numerical simulations.

Similarity solutions have also been investigated in the context of core-collapse supernovae (Goldreich & Weber 1980; Yahil 1983), where the equation of state of the collapsing iron core can be approximated by that of a polytrope, $p = K\rho^{\gamma}$, where K is a constant and $\gamma \simeq 4/3$. (In fact, the effective γ is about 1.3 from the onset of electron capture to the neutrino trapping density, i.e., for 4×10^9 g cm$^{-3} \lesssim \rho \lesssim 10^{12}$ g cm^{-3}; γ becomes close to $4/3$ when $\rho \gtrsim 10^{12}$ g cm^{-3} until nuclear density is reached.) Goldreich & Weber (1980) studied the special case of $\gamma = 4/3$, which provides a

---

[2]We note that Whitworth & Summers (1985) have found a continuum of similarity solutions by relaxing the analyticity condition of the flow at the transonic point; However, these generalized solutions are locally unstable (Hunter 1986; Ori & Piran 1988), and therefore may not be realized in astrophysical situations. We also mention that Boily and Lynden-Bell (1995) have constructed similarity solutions for the gravitational collapse of radiatively cooling gas spheres (with emissivity having a power-law dependence on density and temperature).

good description for the inner homologous core; They also performed a global perturbation analysis and showed that the inner core is stable against all radial and nonradial perturbations. Yahil (1983) generalized the Goldreich-Weber solution to general $\gamma \leq 4/3$; this allows for a proper description of the outer core which collapses supersonically. Since Yahil's solution is the same as the Larson-Penston solution except for different values of γ, we shall often refer them as Larson-Penston-Yahil solutions in the remainder of this paper.

The similarity solutions described above (in both star formation and supernova contexts) assume idealized spherical flows. A realistic gas cloud, however, contains nonradial (nonspherical) perturbations,[3] and it is of interest to understand the behaviors of these perturbations during the collapse/accretion of the cloud. In general, multi-dimensional hydrodynamical simulations are needed to follow the evolution of the perturbed flow, especially when the perturbations become nonlinear. The large dynamical range involved in a collapse makes such simulations particularly challenging (e.g., star formation ultimately involves collapse from $\rho \lesssim 10^{-19}$ g cm^{-3} to $\rho \gtrsim 0.1$ g cm^{-3}; even the initial isothermal collapse stage involves seven orders of magnitude increase in densities; see Truelove et al. 1997,1998 and Boss 1998 for a discussion on the numerical subtleties). An alternative, complementary approach is to carry out linear stability analysis to determine whether the flow is unstable to the growth of any nonradial perturbations. Since the unperturbed flow varies in space and time in a self-similar manner, a global analysis is needed to study perturbations which vary on similar scales as the unperturbed flow itself. The stability properties of the flow therefore depend crucially on boundary conditions at different locations of the flow. In this paper we perform global stability analysis for Larson-Penston-Yahil solutions (general γ) and for Shu's expansion-wave solution ($\gamma = 1$ only) to determine whether these similarity flows contain growing nonradial modes.

While the stability properties of isothermal similarity collapse solutions (the Larson-Penston solution and the expansion-wave solution) are relevant to the formation of binary (and multiple) stars (see §5), the present study stems from our attempts to understand the origin of asymmetric supernovae and pulsar kicks (Goldreich, Lai & Sahrling 1996; see also Lai 1999). Numerical simulations indicate that local hydrodynamical instabilities in the collapsed stellar core (e.g., Burrows et al. 1995; Janka & Müller 1994, 1996; Herant et al. 1994), which can in principle lead to asymmetric matter ejection and/or asymmetric neutrino emission, are not adequate to account for kick velocities $\gtrsim 100$ km s^{-1} (Burrows & Hayes 1996; Janka 1998). Global asymmetric perturbations of presupernova cores may be required to produce the observed kicks. Goldreich et al. (1996) suggested that overstable g-modes driven by shell nuclear burning may provide seed perturbations which could be amplified during core collapse (see also Lai & Goldreich 2000). While the analysis of Goldreich & Weber (1980) shows that the inner homologous core is stable against nonradial

---

[3]A realistic flow may also contain a non-negligible amount of angular momentum and magnetic fields — these are neglected in the main text of this paper. In Appendix A we discuss the perturbative effects of rotation on Larson-Penston-Yahil solutions. Terebey, Shu & Cassen (1984) have considered how slow rotation affects the expansion-wave solution, and Galli & Shu (1993a,b) have studied the perturbative effects of magnetic fields (see also Li & Shu 1997).

perturbations, the situation is not so clear for the supersonically collapsing outer core where pressure plays a less important role. It is therefore important to analyse the global stability of Yahil's self-similar solution. Hanawa & Matsumoto (1999) have recently found a globally unstable bar mode in the pre-collapse Larson-Penston solution (for isothermal collapse). Our independent calculations confirm their result for $\gamma = 1$. Since the analysis of Hanawa & Matsumoto is restricted to perturbations with real eigenvalues and eigenfunctions (see §3), it is not clear whether there exists any other growing modes, nor is it clear whether the growing bar-mode persists for general values of γ (see also Hanawa & Matsumoto 2000a).

The remainder of this paper is organized as follows. Section 2 summarizes the basic properties of the (unperturbed) Larson-Penston-Yahil similarity solution. This serves as a preparation for our stability analysis presented in Section 3. (For readers not interested in technical details, the main results are given in §3.4 and Figures 3-5.) In Section 4 we show that Shu's expansion-wave solution for isothermal collapse is unstable to nonradial perturbations of all angular orders. Finally, we discuss the astrophysical implications of our results in §5. Appendix A contains a discussion of the rotational and vortex modes of Larson-Penston-Yahil solutions.

2. Spherical Larson-Penston-Yahil Self-Similar Collapse

Here we briefly review the (pre-collapse) Larson-Penston-Yahil similarity solutions for spherical collapse and summarize the basic flow properties which are needed for our perturbation analysis (§3).

We adopt a barotropic equation of state, where pressure p and density ρ are related by $p = K\rho^\gamma$, and K and γ are constants. To have gravitational collapse we require $\gamma \leq 4/3$. The two dimensional parameters of the problem are K and the Newton's constant G, from which we can construct a unique similarity variable

$$\eta = \frac{r}{R(t)}, \qquad R(t) = K^{1/2} G^{(1-\gamma)/2} (-t)^{(2-\gamma)}, \tag{1}$$

where r is the spherical radius, and the time t is measured from the epoch of core formation (i.e., the center formally collapses to a singularity at $t = 0$). Our analysis in §3 will be restricted to the pre-collapse solutions, so the domain of interest corresponds to $t < 0$. From dimensional consideration, we can write the dynamical (dependent) variables of the flow in self-similar forms:

$$\rho(r,t) = \rho_t D(\eta), \qquad \rho_t = G^{-1}(-t)^{-2} \tag{2}$$

$$v(r,t) = v_t V(\eta), \qquad v_t = K^{1/2} G^{(1-\gamma)/2}(-t)^{1-\gamma} \tag{3}$$

$$p(r,t) = p_t P(\eta), \qquad p_t = K G^{-\gamma}(-t)^{-2\gamma} \tag{4}$$

$$\psi(r,t) = \psi_t \Psi(\eta), \qquad \psi_t = K G^{1-\gamma}(-t)^{2(1-\gamma)} \tag{5}$$

$$m(r,t) = m_t M(\eta), \qquad m_t = K^{3/2} G^{(1-3\gamma)/2}(-t)^{4-3\gamma} \tag{6}$$

$$u(r,t) = u_t U(\eta), \qquad u_t = K G^{1-\gamma}(-t)^{3-2\gamma}. \tag{7}$$

Here $v(r,t)$ is the radial velocity, $\psi(r,t)$ is the gravitational potential and $m(r,t)$ is the mass interior to radius r; For later purpose, we have defined the velocity stream function u such that $\mathbf{v} = \nabla u$, and $V(\eta) = dU/d\eta = U'$; here and hereafter we shall use prime (') to denote $d/d\eta$. In terms of the dimensionless variables, the equation of state is simply $P = D^\gamma$. The continuity equation, Euler equation and Poisson equation become

$$WD' + DV' + 2D\left(1 + \frac{V}{\eta}\right) = 0, \tag{8}$$

$$\gamma D^{\gamma-2}D' + WV' + (\gamma - 1)V + \frac{M}{\eta^2} = 0, \tag{9}$$

$$M' = 4\pi\eta^2 D, \tag{10}$$

where we have used the relation $M = \eta^2\Psi'$ and have defined

$$W \equiv V + (2 - \gamma)\eta. \tag{11}$$

Note $v_t W = v - (dR/dt)\eta$ is simply the "peculiar" flow velocity with respect to the homologous frame. Equation (8) can be integrated out, with the help of equation (10), to give

$$4\pi\eta^2 DW = (4 - 3\gamma)M. \tag{12}$$

Eliminating V' from equations (8) and (9), we obtain

$$D' = D\left[(1 - \gamma)W - \frac{2W^2}{\eta} + \frac{M}{\eta^2} - (\gamma - 1)(2 - \gamma)\eta\right]\left(W^2 - \gamma D^{\gamma-1}\right)^{-1}. \tag{13}$$

We see there is a sonic point at $\eta = \eta_s$, where $W^2 = \gamma D^{\gamma-1}$, i.e., the (dimensionless) peculiar velocity W equals the sound speed $(\gamma D^{\gamma-1})^{1/2}$.

Equations (10), (12) and (13) determine the spherical self-similar flow. Some properties of the flow are as follows. For $\eta \to 0$:

$$D \to D_0, \qquad V \to -\frac{2}{3}\eta, \qquad M \to \frac{4\pi}{3}D_0\eta^3; \tag{14}$$

For $\eta \to \infty$:

$$D \propto \eta^{-2/(2-\gamma)}, \qquad V \propto \eta^{(1-\gamma)/(2-\gamma)}, \qquad V/A \to \mathcal{M}_\infty = \text{constant}. \tag{15}$$

The physical solution is obtained by adjusting D_0 so that the flow passes through the sonic point smoothly. To obtain accurate transonic solution, it is useful to analyse the behavior of the flow near the sonic point. The values of $D_s = D(\eta_s)$, $W_s = W(\eta_s)$ and $M_s = M(\eta_s)$ are completely determined by requiring both the denominator and numerator of equation (13) to vanish at η_s. For $\epsilon = (\eta - \eta_s)/\eta_s \ll 1$, let $D = D_s(1 + \alpha\epsilon)$ and $W = W_s(1 + \beta\epsilon)$. From equations (10) and (12), we

find $M = M_s[1 + (2 + \alpha + \beta)\epsilon]$ and $2 + \alpha + \beta = (\eta_s/W_s)(4 - 3\gamma)$. Taylor expansion of equation (13) around η_s then yields

$$(\gamma + 1)\alpha^2 - \left[(9 - 7\gamma)\frac{\eta_c}{W_s} - 8\right]\alpha + 2 - (\gamma - 1)(2 - \gamma)\frac{\eta_s^2}{W_s^2}$$
$$+ \left[(4 - 3\gamma)\frac{\eta_s}{W_s} - 2\right]\left[\frac{M_s}{\eta_s W_s^2} + (1 - \gamma)\frac{\eta_s}{W_s} - 4\right] = 0. \tag{16}$$

For $\gamma = 1$, the two roots are $\alpha = -1$ and $\alpha = \eta_s - 3$, and the former gives the Larson-Penston solution. For general γ, the smaller of the two roots of (16) corresponds the Yahil-Larsen-Penston solution, which is the only solution with $|V|$ supersonic at large η (this is called type II solution by Hunter 1977). The other root gives rise to a infinite (but discrete) number of solutions which are subsonic in $|V|$ at large η (called Type I by Hunter). We will not discuss these type I solutions further in this paper since they are strongly unstable against radial perturbations (Hanawa & Nakayama 1997). Our numerical procedure for finding the transonic solution is as follows: Guess D_0 and η_s; Using the boundary conditions given above, integrate equations (10) and (13) outward from $\eta = 0$ and inward from η_s to a middle point η_{mid}; Using the Newton-Raphson scheme (Press et al. 1992) to vary D_0 and η_s so that the two integrations match at η_{mid}.

Figure 2 gives two examples of the Larson-Penston-Yahil self-similar solutions of spherical collapse (for $\gamma = 1$ and 1.3). For convenience, we list in Table 1 the key parameters of the solutions for different values of γ.

3. Perturbations of Larson-Penston-Yahil Collapse Solution

Our stability analysis relies on calculating the global linear modes of the self-similar flow. In general, it is not meaningful to speak of modes in flows where the unperturbed state is time dependent. Self-similar flows constitute an exception, since the spatial structure of the unperturbed flow is constant in shape, although not in scale. In this case, a mode represents a linearized disturbance with shape-preserving spatial structure and power-law time dependence relative to the unperturbed flow. The mode structure and stability depend on the feedback between boundary conditions at different locations of the flow.

3.1. Perturbation Equations

We consider flows with no net angular momentum and vorticity.[4] The fluid velocity is completely specified by the stream function (velocity potential), i.e., $\mathbf{v} = \nabla u$. The continuity equation,

---

[4]When rotation is a small perturbation, it is decoupled from the density perturbation and the potential flow. We discuss the rotational perturbations of self-similar flows in Appendix A.

Euler equation and Poisson equation for the irrotational flow can be written as

$$\frac{\partial \rho}{\partial t} + \nabla \cdot (\rho \nabla u) = 0, \tag{17}$$

$$\frac{\partial u}{\partial t} + \frac{1}{2}(\nabla u)^2 + h + \psi = 0, \tag{18}$$

$$\nabla^2 \psi = 4\pi G \rho, \tag{19}$$

where the enthalpy $h = \int dP/\rho = \gamma K \rho^{\gamma-1}/(\gamma - 1)$ for $\gamma \neq 1$ and $h = K \ln \rho$ for $\gamma = 1$. The perturbed hydrodynamical equations are

$$\frac{\partial}{\partial t}\delta \rho + \frac{1}{r^2}\frac{\partial}{\partial r}\left(r^2 \delta \rho \frac{\partial u}{\partial r}\right) + \frac{\partial \rho}{\partial r}\frac{\partial \delta u}{\partial r} + \rho \nabla^2 \delta u = 0, \tag{20}$$

$$\frac{\partial}{\partial t}\delta u + v\frac{\partial \delta u}{\partial r} + \gamma K \rho^{\gamma-2}\delta \rho + \delta \psi = 0, \tag{21}$$

$$\nabla^2 \delta \psi - 4\pi G \delta \rho = 0, \tag{22}$$

where $\delta \rho$, δu and $\delta \psi$ are the Eulerian perturbations of density, velocity potential and gravitational potential, respectively. Separating out the angular dependence in terms of spherical harmonics Y_{lm}, we write the perturbations in the form

$$\delta \rho(\mathbf{r}, t) = (-t)^s \rho_t \, \delta D(\eta) Y_{lm}, \tag{23}$$

$$\delta u(\mathbf{r}, t) = (-t)^s u_t \, \delta U(\eta) Y_{lm}, \tag{24}$$

$$\delta \psi(\mathbf{r}, t) = (-t)^s \psi_t \, \delta \Psi(\eta) Y_{lm}, \tag{25}$$

where ρ_t, ψ_t and u_t are given by equations (2), (5) and (7). The velocity perturbation is given by

$$\delta \mathbf{v}(\mathbf{r}, t) = \nabla \delta u(\mathbf{r}, t) = (-t)^s v_t \left[\delta V_r(\eta)\,\hat{r} + \delta V_\perp(\eta)\hat{\nabla}_\perp\right] Y_{lm}, \tag{26}$$

where

$$\hat{\nabla}_\perp \equiv \hat{\theta}\frac{\partial}{\partial \theta} + \frac{\hat{\phi}}{\sin \theta}\frac{\partial}{\partial \phi}, \tag{27}$$

and the dimensionless radial and tangential velocity perturbations are

$$\delta V_r(\eta) = \delta U'(\eta), \qquad \delta V_\perp(\eta) = \frac{\delta U(\eta)}{\eta}. \tag{28}$$

In equations (23)-(26), the (unknown) power-law index s constitutes an eigenvalue of the problem. Since $\delta \rho(\mathbf{r}, t)/\rho(r, t) = (-t)^s [\delta D(\eta)/D(\eta)] Y_{lm}$ (and similarly for other variables), the value of s determines the global behavior of the perturbation relative to the unperturbed flow: The perturbation is globally unstable if the real part of s, $\mathrm{Re}(s)$, is less than zero, and it is stable if $\mathrm{Re}(s) > 0$. Substituting (23)-(25) into equations (20)-(22), we have

$$W\delta D' + D\delta U'' + \left(2 - s + V' + \frac{2}{\eta}V\right)\delta D + \left(D' + \frac{2}{\eta}D\right)\delta U' - \frac{l(l+1)}{\eta^2}D\delta U = 0, \tag{29}$$

$$W\delta U' + \gamma D^{\gamma-2}\delta D + (2\gamma - 3 - s)\delta U + \delta \Psi = 0, \tag{30}$$

$$\delta \Psi'' = \frac{l(l+1)}{\eta^2}\delta \Psi - \frac{2}{\eta}\delta \Psi' + 4\pi \delta D. \tag{31}$$

We can eliminate $\delta U''$ from (29) using (30) to obtain

$$\left(W^2 - \gamma D^{\gamma-1}\right)\frac{\delta D'}{D} = -(3 - 3\gamma + s - 2V')\delta U'$$
$$- \left[\left(2 - s + V' + \frac{2}{\eta}V\right)WD^{-1} - \gamma(\gamma - 2)D^{\gamma-3}D'\right]\delta D$$
$$+ \frac{l(l + 1)}{\eta^2}W\delta U + \delta\Psi'. \tag{32}$$

Thus the perturbation equation is singular at the sonic point ($\eta = \eta_s$). Equations (30)-(32) are the basic equations for the eigenvalue problem.

3.2. Boundary Conditions

To solve for the eigenvalue s, we need to know the boundary conditions. Since the unperturbed flow is regular at $\eta \to 0$, we require the perturbations to be regular also. This gives, for $\eta \to 0$,

$$\delta D = \delta D_0\eta^l, \qquad \delta U = \delta U_0\eta^l, \qquad \delta\Psi = \delta\Psi_0\eta^l, \qquad (\eta \to 0) \tag{33}$$

where the three constants δD_0, δU_0 and $\delta\Psi_0$ are related by

$$\gamma D_0^{\gamma-2}\delta D_0 = -\left[\left(\frac{4}{3} - \gamma\right)l - 3 + 2\gamma - s\right]\delta U_0 - \delta\Psi_0. \tag{34}$$

Since the unperturbed flow is nearly static ($V \to 0$) at $\eta \to 0$, the conditions (33)-(34) are similar to those applied for nonradial pulsations in stars (e.g., Unno et al. 1989).

The boundary conditions at $\eta \to \infty$ are trickier. Let $\delta D \propto \eta^a$, $\delta U \propto \eta^b$ and $\delta\Psi \propto \eta^c$ for $\eta \to \infty$. There are four independent solutions to the fourth order systems of differential equations. Using the scaling relations in (15), we find that the values of a, b, c for the four solutions are

$$\text{Solution I}: \qquad a = \frac{s - 2}{2 - \gamma}, \qquad b = c = a + 2 = \frac{s + 2(1 - \gamma)}{2 - \gamma}; \tag{35}$$

$$\text{Solution II}: \qquad a = \frac{s - 3}{2 - \gamma}, \qquad b = \frac{s + 3 - 2\gamma}{2 - \gamma}, \qquad c = a + 2 = \frac{s + 1 - 2\gamma}{2 - \gamma}; \tag{36}$$

$$\text{Solution III}: \qquad a = -l - 3 - \frac{2}{2 - \gamma}, \qquad b = c = -(l + 1); \tag{37}$$

$$\text{Solution IV}: \qquad a = l - 2 - \frac{2}{2 - \gamma}, \qquad b = c = l. \tag{38}$$

For each solution, the ratio $\delta U/\delta\Psi$ and $\delta D/\delta\Psi$ are uniquely determined. The general solution of equations (30)-(32) is a superposition of Solution I-IV. In Solution I and II, the potential perturbation $\delta\Psi$ is produced by local density perturbation δD (thus $c = a + 2$); In Solution III, $\delta\Psi$ at a large η is produced by a multipole moment associated with δD at smaller η. Solutions I-III are physically allowed. Solution IV, however, is not arrowed, since it corresponds to the situation where $\delta\Psi$ at

a given (large) η is produced by density perturbation at even larger η, and $\delta\Psi$ increases without bound as $\eta \to \infty$. Therefore, the eigenmode at larger η is a linear combination of Solution I,II and III. Unless the Re(s) is extremely negative, i.e., for Re(s) $> -(4 - 3\gamma) - (2 - \gamma)l$, the behaviors of δD and $\delta\Psi$ at large η are dominated by Solution I, while the behavior of δU is dominated by Solution II. Thus we have

$$\frac{\delta D}{D}, \ \frac{\delta U}{U}, \ \frac{\delta\Psi}{\Psi} \propto \eta^{s/(2-\gamma)}, \tag{39}$$

where we have used $U \sim \eta V \propto \eta^{(3-2\gamma)/(2-\gamma)}$ and $\Psi \sim \eta^2 D \propto \eta^{2(1-\gamma)/(2-\gamma)}$ at $\eta \to \infty$. In practice, we implement the outer boundary condition at large η as

$$\delta\Psi' = \frac{c}{\eta}\delta\Psi, \qquad c = \frac{s + 2(1 - \gamma)}{2 - \gamma} \qquad (\eta \to \infty). \tag{40}$$

Equation (39) indicates that when Re(s) > 0, the fractional perturbations $\delta D/D$, $\delta U/U$ and $\delta\Psi/\Psi$ diverge as η increases to infinity. Thus only for globally unstable modes (Re(s) < 0) are the fractional perturbations finite at $\eta \to \infty$. Whether such an unstable mode exists (for a given l and γ) is unknown *a priori*. Note that equation (39) also corresponds to

$$\frac{\delta\rho(\mathbf{r}, t)}{\rho(r, t)}, \ \frac{\delta u(\mathbf{r}, t)}{u(r, t)}, \ \frac{\delta\psi(\mathbf{r}, t)}{\psi(r, t)} \propto r^{s/(2-\gamma)}(-t)^0, \tag{41}$$

i.e., the perturbations are independent of time for $\eta \to \infty$.

Since the sonic point ($\eta = \eta_s$) is a singular point of equation (32), another crucial condition for the perturbation analysis is that the perturbations remain regular and pass through the sonic point smoothly.

3.3. Numerical Method

Our numerical procedure for finding an eigenmode is as follows: (i) We first guess s and $\delta U_0/\delta\Psi_0$ (note that in general they are complex), and use equation (34) to find $\delta D_0/\delta\Psi_0$; (In plotting the eigenfunctions below, we adopt the normalization such that $\delta\Psi_0 = 1$); (ii) We then integrate equations (30)-(32) from a small $\eta_{\rm in} \ll 1$ to η_s and then from η_s to a large $\eta_{\rm out}$ (we typically choose $\eta_{\rm out} = 10^3 - 10^4$); (iii) Using a Newton-Raphson scheme (Press et al. 1992), we vary the values of s and $\delta U_0/\delta\Psi_0$ until the right-hand side of equation (32) vanishes at η_s and condition (40) is satisfied at $\eta_{\rm out}$. Note that in step (ii), we first integrate the equations to $\eta_{s-} = \eta_s(1 - \varepsilon)$, where $0 < \varepsilon \ll 1$ (we typically choose $\varepsilon = 10^{-4} - 10^{-3}$), and advance the solution to η_s and to $\eta_{s+} = \eta_s(1 + \varepsilon)$ using the derivatives evaluated at η_{s-}, and then continue the integration from η_{s+} to $\eta_{\rm out}$. We have found that this procedure works well except that for some high-order modes the convergence of the eigenvalue s as ε decreases requires very small ε. We have also tried using derivatives evaluated at η_s (and using L'Hôpital's rule to calculate $\delta D'$ at η_s) to advance the solution from η_{s-} to η_{s+}, but this did not lead to significant improvement. Ideally, one should not integrate

"into" the singular point η_s, but rather should integrate from η_s inward to a midpoint η_{mid} ($< \eta_s$) and match the solution there. However, this introduces several additional unknown parameters and makes the multi-dimensional Newton-Raphson scheme difficult to converge in practice.

3.4. Results

We first note that for $l = 1$, the lowest-order mode (the one with no node in the radial eigenfunction) is a trivial solution; it corresponds to choosing the origin of the coordinates away from the center of the spherical flow. The eigenfunctions are $\delta D = D'$, $\delta U = U'$, $\delta \Psi = \Psi'$. The negative eigenvalue $s = \gamma - 2$ should not be considered as an indication of global instability. All other nonradial modes are nontrivial.

3.4.1. Unstable Modes

For $\gamma = 1$ and $l = 2$, we find that the lowest-order mode has a real eigenvalue, $s = -0.352$. Figure 3 depicts the eigenfunctions of the mode. Near the center ($\eta \to 0$), we find $\delta U_0/\delta \Psi_0 = -0.836$. The eigenfunctions are well-behaved everywhere, and go through the transonic point η_s smoothly. The negative eigenvalue s indicates that the bar-mode is globally unstable, with

$$\frac{\delta \rho(\mathbf{r}, t)}{\rho(r, t)} = (-t)^{-0.352} \left[\frac{\delta D(\eta)}{D(\eta)} \right] Y_{2m}, \tag{42}$$

$$\frac{\delta \mathbf{v}(\mathbf{r}, t)}{v(r, t)} = (-t)^{-0.352} \left[\frac{\delta V_r(\eta)}{V(\eta)} \hat{r} + \frac{\delta V_\perp(\eta)}{V(\eta)} \hat{\nabla}_\perp \right] Y_{2m}, \tag{43}$$

where $\rho(r, t)$ and $v(r, t)$ specify the unperturbed spherical flow, and $\delta V_r(\eta) = \delta U'(\eta)$, $\delta V_\perp(\eta) = \delta U(\eta)/\eta$. Figure 4 illustrates the growth of the density perturbation as the collapse proceeds. The fractional perturbation grows as $(-t)^{-0.352} \propto \rho_c(t)^{0.176}$, where $\rho_c(t) = \rho(0, t)$ is the central density of the cloud. The growing bar-mode corresponds to the deformation of the collapsing cloud toward an ellipsoidal shape. Depending on the initial perturbations, the deformed cloud may take the form of an oblate disk or a prolate bar (see also Hanawa & Matsumoto 1999).

As γ increases, the mode tends to be stablized by the effect of pressure. Figure 5 depicts the variation of $s = s_0$ for the lowest-order bar-mode ($l = 2$) as a function of γ. We find that s increases with increasing γ, and the mode is unstable (with negative s) only for $\gamma \leq 1.09$.[5] Figure 6 gives a few examples of the mode eigenfunctions for several different values of γ.

[5]Similar result is also obtained by Hanawa & Matsumoto (2000a) in a different analysis. The author thanks the referee, T. Hanawa, for pointing out this paper.

3.4.2. Stable Modes

We have searched numerically for other unstable modes [with $\mathrm{Re}(s) < 0$] for $1 \le \gamma \le 4/3$ and $l = 1, 2, 3, \cdots$. Our search covers the domain $-5 \lesssim \mathrm{Im}(s) \lesssim 5$. However, except for those discussed in §3.4.1, all modes we have found are stable [with $\mathrm{Re}(s) > 0$]. As an example, the dashed curve in Fig. 6 shows the eigenfunction of a high-order $l = 2$ mode (for $\gamma = 1$), with $s_1 = 0.23 + 0.26i$. Note that as γ increases, the ordering of the modes can change. This is seen from Figure 5: For $\gamma \lesssim 1.11$ we have $s_0 < \mathrm{Re}(s_1)$, but for $\gamma \gtrsim 1.11$ we find $s_0 > \mathrm{Re}(s_1)$. We have not explored the spectrum of high-order modes in detail, since these modes are all stable. Moreover, as the fractional perturbations associated with the stable modes diverge in the $\eta \to \infty$ limit (see eq. [39]), these modes are only formally well-defined, but are of no physical importance.

4.   Perturbations of "Inside-Out" Collapse of Isothermal Cloud

In this section we present our perturbation analysis of Shu's expansion-wave solution which describes the "inside-out" collapse of a isothermal gas cloud. The equation of state is $p = K\rho = \rho a^2$, where a is the sound speed.

4.1.   Spherical Inside-Out Collapse: Shu's Expansion-Wave Solution

The expansion-wave solution describes the post-collapse $(t > 0)$ evolution of the flow. The similarity variable is defined as

$$\eta = \frac{r}{at}. \tag{44}$$

The flow variables can be written in self-similar forms as in equations (2)-(7), except that in ρ_t, v_t, p_t, $\cdots$ we have to replace $(-t)$ by t and set $\gamma = 1$, i.e.,

$$\rho_t = \frac{1}{4\pi G t^2}, \quad v_t = a, \quad p_t = \frac{a^2}{Gt^2}, \quad \psi_t = a^2, \quad m_t = \frac{a^3 t}{G}, \quad u_t = a^2 t. \tag{45}$$

(Note that to follow Shu's convention, we have included the factor 4π in ρ_t.) In terms of the similarity variables, the continuity equation, Euler equation, and Poisson equation are

$$(V - \eta)D' + DV' + 2D\left(\frac{V}{\eta} - 1\right) = 0, \tag{46}$$

$$\frac{D'}{D} + (V - \eta)V' + \frac{M}{\eta^2} = 0, \tag{47}$$

$$M' = \eta^2 D. \tag{48}$$

These equations can be rearranged into the standard form as given by Shu:

$$[(V - \eta)^2 - 1]\frac{D'}{D} = (\eta - V)\left[D - 2\left(1 - \frac{V}{\eta}\right)\right], \tag{49}$$

$$\left[(V - \eta)^2 - 1\right] V' = (\eta - V)\left[D(\eta - V) - \frac{2}{\eta}\right], \tag{50}$$

and $M = \eta^2(\eta - V)D$.

Some properties of the expansion-wave solution are as follows. For $\eta > 1$, the solution describes a static isothermal sphere, with $V(\eta) = 0$ and $D(\eta) = 2/\eta^2$. The surface $\eta = 1$ is the rarefaction (expansion) wave front. For $\eta \to 0$, the solution describes a free-fall, with $M \to M_0 = 0.975$, $V \to -\left(2M_0/\eta\right)^{1/2}$, and $D \to \left(M_0/2\eta^3\right)^{1/2}$. While D and V are continuous at $\eta = 1$, D' and V' are not:

$$V'(1+) = 0, \quad D'(1+) = -4; \qquad V'(1-) = 1, \quad D'(1-) = -2. \tag{51}$$

(The notation $\eta = 1+$ means that $\eta \to 1$ from above, and $\eta = 1-$ means $\eta \to 1$ from below.)

4.2. Perturbation Equations

As in equations (23)-(25), we consider perturbations of the form

$$\delta\rho(\mathbf{r}, t) = t^s \rho_t \, \delta D(\eta) Y_{lm}, \tag{52}$$

$$\delta u(\mathbf{r}, t) = t^s u_t \, \delta U(\eta) Y_{lm}, \tag{53}$$

$$\delta\psi(\mathbf{r}, t) = t^s \psi_t \, \delta\Psi(\eta) Y_{lm}. \tag{54}$$

Since $\delta\rho(\mathbf{r}, t)/\rho(r, t) = t^s \left[\delta D(\eta)/D(\eta)\right] Y_{lm}$ (and similarly for other variables), the power-law index s specifies the evolution of the perturbation relative to the background: The flow is unstable if $\mathrm{Re}(s) > 0$ and stable if $\mathrm{Re}(s) < 0$. Substituting (52)-(54) into the perturbation equations (20)-(22), we obtain

$$(V - \eta)\delta D' + D\delta U'' + \left(-2 + s + V' + \frac{2}{\eta}V\right)\delta D + \left(D' + \frac{2}{\eta}D\right)\delta U' - \frac{l(l+1)}{\eta^2}D\delta U = 0, \tag{55}$$

$$(V - \eta)\delta U' + \frac{\delta D}{D} + (1 + s)\delta U + \delta\Psi = 0, \tag{56}$$

$$\delta\Psi'' + \frac{2}{\eta}\delta\Psi' - \frac{l(l+1)}{\eta^2}\delta\Psi - \delta D = 0. \tag{57}$$

We can use equation (56) to eliminate $\delta U''$ in equation (55) and obtain

$$\left[(V - \eta)^2 - 1\right]\frac{\delta D'}{D} - (2V' + s)\delta U' + \left[\left(-2 + s + V' + \frac{2}{\eta}V\right)(V - \eta) + \frac{D'}{D}\right]\frac{\delta D}{D}$$

$$- \frac{l(l+1)}{\eta^2}(V - \eta)\delta U - \delta\Psi' = 0. \tag{58}$$

Thus, the expansion-wave front ($\eta = 1$) is a singular point of the perturbation equation. Also, equation (57) can be written in the integral form:

$$\delta\Psi(\eta) = -\eta^l P(\eta) - \frac{Q(\eta)}{\eta^{l+1}}, \tag{59}$$

where

$$P(\eta) \;=\; \frac{1}{2l+1} \int_{\eta}^{\infty} \eta'^{\,1-l} \delta D(\eta')\, d\eta', \qquad P' = -\frac{1}{2l+1} \eta^{1-l} \delta D, \tag{60}$$

$$Q(\eta) \;=\; \frac{1}{2l+1} \int_{0}^{\eta} \eta'^{\,l+2} \delta D(\eta')\, d\eta', \qquad Q' = \frac{1}{2l+1} \eta^{l+2} \delta D. \tag{61}$$

4.3. Series Solution for $\eta > 1$

For $\eta > 1$, we have $V = 0$ and $D = 2/\eta^2$, the perturbation equations can be solved in Frobenius series. We consider the solution which satisfies $\delta D/D \to 0$, $\delta U \to 0$, and $\delta \Psi \propto \eta^{-l-1} \to 0$ for $\eta \to \infty$ (i.e., $\delta \Psi$ is given by the decreasing solution of the Laplace equation);[6] The last condition implies that Q approaches a constant as $\eta \to \infty$. Thus we can write

$$Q(\eta) = \sum_{n=0}^{\infty} q_{2n} \eta^{-2n}. \tag{62}$$

Equation (61) then gives

$$\delta D(\eta) = \sum_{n=0}^{\infty} d_{2n} \eta^{-2n-l-3}, \qquad d_{2n} = -2n(2l+1)\, q_{2n}. \tag{63}$$

Using equations (59), (60) and requiring $P \to 0$ as $\eta \to \infty$, we have

$$\delta \Psi(\eta) = \sum_{n=0}^{\infty} \psi_{2n} \eta^{-2n-l-1}, \qquad \psi_{2n} = -\frac{2l+1}{2n+2l+1}\, q_{2n}. \tag{64}$$

Substituting (63) and (64) into (56) yields

$$\delta U(\eta) = \sum_{n=0}^{\infty} u_{2n} \eta^{-2n-l-1}, \qquad u_{2n} = \frac{(2l+1)(2n^2+2ln+n+1)}{(2n+2l+1)(2n+l+2+s)}\, q_{2n}. \tag{65}$$

Finally, using equation (58), we obtain the recurrence relation:

$$(2n+3+l+s)d_{2n+2} = (2n+l+1)d_{2n} + 2\left[s(2n+l+1) + l(l+1)\right] u_{2n}$$
$$+2(2n+l+1)\psi_{2n} \qquad\qquad (n = 0, 1, 2, \cdots) \tag{66}$$

With this recurrence relation, the complete solution for $\eta > 1$ can be obtained. Note that for $\eta \to \infty$, the asymptotic scalings of the perturbations are

$$\delta \Psi \to \frac{q_0}{\eta^{l+1}}, \qquad \delta U \to \frac{q_0}{(l+2+s)\eta^{l+1}}, \qquad \delta D \propto \frac{1}{\eta^{l+5}}. \tag{67}$$

---

[6]The fourth order system of differential equations allows for four independent solutions, but this solution (which must exist for any physical situation) alone is adequate for our stability analysis (§4.4).

4.4. Instability

Here we use the series solution of §4.3 and the boundary condition at the expansion-wave front ($\eta = 1$) to show that Shu's solution is unstable. As equation (58) indicates, the expansion-wave front is a singular point of the perturbation equation. A natural (necessary) boundary condition at $\eta = 1$ is that the perturbation is finite (although δD and $\delta V_r = \delta U'$ can be discontinuous across $\eta = 1$; see below).

We can examine the behavior of the perturbation at $\eta \to 1+$ using the series solution of §4.3. From the recurrence relation (66) we find, for $n \to \infty$,

$$\frac{d_{2n+2}}{d_{2n}} \to 1 - \frac{1+s}{n}, \tag{68}$$

$$\frac{u_{2n+2}}{u_{2n}} \to 1 - \frac{2+s}{n}, \tag{69}$$

$$\frac{\psi_{2n+2}}{\psi_{2n}} \to 1 - \frac{3+s}{n}. \tag{70}$$

Thus in order for δD to be finite at $\eta \to 1+$, we require $\mathrm{Re}(s) > 0$ (e.g., Mathews & Walker 1970). One can similarly show that in order for $\delta V_r = \delta U'$ to be finite at $\eta \to 1+$, we require $\mathrm{Re}(s) > 0$. Thus, any perturbations which are well-behaved at the expansion-wave front must be globally unstable.

A possible caveat in the analysis given above is that in the presence of flow perturbations, the rarefaction front is also perturbed, and $\delta D(\eta \to 1+)$ does not give the density perturbation at the perturbed expansion-wave front; one might therefore be concerned that the divergence of $\delta D(\eta \to 1+)$ is a result of an improper definition of δD. To address this problem, we define a stretched radial coordinate via

$$\xi(\eta) = \eta \left(1 + \Delta Y_{lm} t^s\right), \tag{71}$$

where Δ is a constant (to be determined). The perturbed rarefaction front is located at $\xi(\eta = 1)$. Since $D(\eta) + \delta D(\eta) Y_{lm} t^s = D[\xi(\eta)] + \delta D[\xi(\eta)] Y_{lm} t^s$, we have

$$\delta D[\xi(\eta)] = \delta D(\eta) - \eta D'(\eta)\Delta. \tag{72}$$

Similarly, $\delta U'[\xi(\eta)] = \delta U'(\eta) - \eta V'(\eta)\Delta$. Since $\delta D[\xi(\eta)]$ and $\delta U'[\xi(\eta)]$ must be continuous across the rarefaction front, and since D' and V' are discontinuous at $\eta = 1$ (see eq. [51]), we infer that $\delta D(\eta)$ and $\delta V_r(\eta)$ are discontinuous at $\eta = 1$. Evaluating equation (58) at $\eta = 1+$ and $\eta = 1-$, we find

$$\Delta = -\frac{1}{s+1}\delta U'(1+). \tag{73}$$

Using equation (72) we obtain

$$\delta D[\xi(\eta = 1+)] = \delta D(\eta = 1+) - \frac{4}{(s+1)}\delta U'(\eta = 1+). \tag{74}$$

Using the series solution of §4.3, we can easily show that $\delta D[\xi(\eta = 1+)]$ diverges unless $\mathrm{Re}(s) > 0$.

Another concern one might have is that the divergence of δD and δV_r at $\eta = 1+$ discussed above simply indicates that the series expansion breaks down at $\eta = 1$ rather than the actual divergence of the function δD and δV_r. To address this issue, we show in Figure 7 several examples of the absolute value of the density perturbation δD at small $(\eta - 1)$ for several different values of s. The function δD is calculated using the series expansion given in §4.3 (normalized by setting $q_0 = 1$). We see that, in accordance with our discussion above, when $\mathrm{Re}(s) < 0$, the density perturbation δD diverges as $\eta \to 1+$. Indeed, an analysis of the perturbation equations near $\eta = 1+$ shows that for $0 < x \equiv \eta - 1 \ll 1$ the perturbations have the following behavior:

$$\delta D = C_0 x^s \left[1 + \mathcal{O}(x)\right] + C_1 \left[1 + \mathcal{O}(x)\right], \tag{75}$$

$$\delta U = \frac{C_0}{2(s+1)} x^{s+1} \left[1 + \mathcal{O}(x)\right] + C_2 \left[1 + \mathcal{O}(x)\right], \tag{76}$$

$$\delta \Psi = \frac{C_0}{(s+1)(s+2)} x^{s+2} \left[1 + \mathcal{O}(x)\right] + C_3 \left[1 + \mathcal{O}(x)\right], \tag{77}$$

where C_0, C_1, C_2, C_3 are constants. This clearly shows that $\delta D(\eta = 1+)$ diverges for $\mathrm{Re}(s) < 0$ — We could have deduced this result simply by examing the perturbation equations near $\eta = 1+$, except that without the series solution discussed in §4.3 we would not know whether $C_0 = 0$ is a possibility. The numerical results (based on the series solution) depicted in Figure 7 agree with (75)-(77) and $C_0 \neq 0$, i.e., the boundary condition at $\eta \to \infty$ requires $C_0 \neq 0$. It is this global consideration of the perturbations at $\eta \to \infty$ and at $\eta \to 1+$ that forces us to conclude that the expansion-wave solution is unstable to perturbations of all l's.

Note that our analysis above indicates $\mathrm{Re}(s) > 0$, but we have not solved for s. (The actual values of s depend on the flow at $\eta < 1$ and the boundary conditions at $\eta \to 0$.) Thus the growth rates of the instabilities are unknown at present.

5. Discussion

Early studies by Hunter (1962) and by Lin, Mestel & Shu (1965) demonstrated that uniform, pressure-free gas clouds undergoing gravitational collapse are unstable toward fragmentation and shape deformation, with perturbations growing asymptotically as $\delta \rho(\mathbf{r}, t)/\rho(t) \propto (t_0 - t)^{-1} \propto \rho(t)^{1/2}$ in the linear regime, where t_0 denotes the epoch of complete collapse, and $\rho(t)$ is the unperturbed uniform density. However, the presence of even a small initial central concentration and pressure forces significantly alters the evolution of the cloud. If the gas pressure is simply related to the density by a power-law, $p = K \rho^\gamma$ (polytropic equation of state), the flow asymptotically approaches the similarity solutions found by Larson (1969), Penston (1969) (for isothermal gas $\gamma = 1$), by Goldreich & Weber (1980) (for $\gamma = 4/3$), and by Yahil (1983) (for general γ). Since the local Jeans length is of the same order as the length scale at which the flow varies, a global analysis is needed to determine the stability properties of the collapsing cloud. The result (§3) presented in this paper

(see also Hanawa & Matsumoto 1999) shows that for sufficiently soft equation of state ($\gamma \leq 1.09$), the Larson-Penston-Yahil similarity flow is unstable against bar-mode perturbations, such that $\delta\rho(\mathbf{r}, t)/\rho(r, t) \propto (t_0 - t)^s Y_{2m}(\theta, \phi)$ with $s < 0$ ($s = -0.352$ for $\gamma = 1$ and s increases to zero as γ increases to 1.09, see Fig. 5), where t_0 denotes the epoch of core formation. Since the central density increases as $\rho_c(t) \propto (t_0 - t)^{-2}$, the growth of perturbation, $\delta\rho(\mathbf{r}, t)/\rho(r, t) \propto \rho_c(t)^{-s/2}$, is slow (e.g., for isothermal collapse, $\delta\rho/\rho$ increases by a factor of 1.5 when ρ_c increases by a factor of 10). Such a slow growth (compared with the $\delta\rho/\rho \propto \rho^{1/2}$ behavior for the collapse of uniform, pressure-less gas) is a result of the stablizing influence of pressure, despite the large Mach number (about 3) achieved in the outer region of the cloud.

Our stability analysis applies to the pre-collapse stage (prior to core formation) of the Larson-Penston-Yahil solutions. After the central core forms, the outer core and envelope accrete onto it (see Fig. 1). The gas approaches free-fall as $r \to 0$, and the Mach number becomes much greater than unity. In this (accretion) stage, nonradial perturbations (of all scales) grow kinematically as $\delta\rho/\rho \propto r^{-1/2} \propto \rho^{1/3}$, where $r(t)$ is the radius of a fluid element and $\rho(t) \propto r^{-3/2}$ its comoving density (Lai & Goldreich 2000). Although the fluid element is free-falling, the perturbation grows more slowly compared with the case of uniform pressure-less collapse because the steep velocity gradients provide a stablizing influence on the flow.

The global bar-mode instability for isothermal collapse may have important implications for star formation, particularly in connection with the formation of binary (and multiple) stars (see also Hanawa & Matsumoto 1999; Matsumoto & Hanawa 1999). Fragmentation is unlikely to occur in a globally spherical collapse because small condensations do not contract fast enough to separate out from the converging bulk flow. Angular momentum (or magnetic field) can obviously make the cloud nonspherical, and thus facilitate fragmentation (e.g., Burkert & Bodenheimer 1996; Burkert, Bate & Bodenheimer 1997; Truelove et al. 1997,1998; Boss 1998). Observations suggest that many of the molecular cloud cores (with mass of order a few $M_\odot$ and size 0.1 pc) have elongated shapes (Myers et al. 1991) and slow rotation rates (with the ratio of rotational to gravitational energies of order 0.02; Goodman et al. 1993), implying that rotation is probably not a crucial factor in driving fragmentation on scales greater than 200 AU. Our result on the growth of bar-mode perturbations ($\delta\rho \propto Y_{2m}$) indicates that, even without net angular momentum, the collapsing cloud tends to deform into an ellipsoidal shape (oblate disk or prolate bar, depending on which m-mode perturbation is dominant initially). Fragmentation is more likely to occur for such deformed configurations (e.g., Bonnel 1999; Matsumoto & Hanawa 1999).

In the context of core-collapse supernovae, our result shows that the homologous inner core and the supersonic outer core are globally stable against nonradial perturbations prior to core bounce at nuclear density and the formation of the proto-neutron star. However, during the subsequent accretion of the outer core (involving 15% of the core mass) and envelope onto the proto-neutron star, nonspherical perturbations can grow according to $\delta\rho/\rho \propto r^{-1/2}$ or even $\delta\rho/\rho \propto r^{-1}$ (Lai & Goldreich 2000). The asymmetric density perturbations seeded in the presupernova star, especially those in the outer region of the iron core, are therefore amplified during collapse. The enhanced

asymmetric density perturbation may lead to asymmetric shock propagation and breakout, which then give rise to asymmetry in the explosion and a kick velocity to the neutron star (Goldreich et al. 1996; Burrows & Hayes 1996).

Our stability analysis (§4) shows that Shu's expansion-wave solution is globally unstable to perturbations of all l's, although the growth rates are unknown at present. The implication of this result is not entirely clear. It is well-known that a static singular isothermal sphere is highly unstable to radial perturbations (A truncated Bonner-Ebert isothermal sphere is unstable when the range of density from the center to the surface is greater than 14.04; see Bonner 1956, Hunter 1977). Earlier one-dimensional numerical simulations have already shown that a collapsing isothermal cloud does not approach the expansion-wave solution (Hunter 1977; Foster & Chevalier 1993). Our stability analysis corroborates this result, and indicates that the expansion-wave solution cannot be realised in a pure hydrodynamical situation.

Magnetic fields play an important role in the current paradigm for forming low-mass stars (e.g., Shu, Adams & Lizano 1987; Shu et al. 1999; Mouschovias & Ciolek 1999). Ambipolar diffusion of magnetic fields drives the quasi-static contraction of the molecular cloud core with growing central concentration such that the core asymptotically approaches the state of a singular isothermal sphere. When the flux-to-mass ratio drops below certain critical value, a runaway "inside-out" collapse ensues, and it is thought that this collapse is well described by the expansion-wave solution (Shu et al. 1999). In reality, there is probably no sharp distinction between the quasi-static contraction and dynamical collapse (e.g., Safier, McKee & Stahler 1997; Li 1998), and a real singular isothermal sphere can never be reached. Our global stability analysis of the expansion-wave solution (§4) does not depend on the mathematical singularity of the solution at $r = 0$, but depends on the existence of a well-defined rarefaction front and a static isothermal density profile outside the front in the solution. It in not clear whether our idealized hydrodynamical stability analysis can be applied to more realistic situations with (even sub-dominant) magnetic fields (see Galli & Shu 1993a,b and Li & Shu 1997 for the effects of magnetic field on self-similar "inside-out" collapse).

A. Rotational Perturbations in Larson-Penston-Yahil Solutions

A general velocity perturbation can be written as

$$\delta\mathbf{v}(\mathbf{r}, t) = \delta v_r(r, t) Y_{lm} \,\hat{r} + \delta v_\perp(r, t) \hat{\nabla}_\perp Y_{lm} + \hat{\nabla}_\perp \times [\delta v_{\rm rot}(r, t) Y_{lm} \,\hat{r}] . \tag{A1}$$

Using Euler equation, we obtain

$$\frac{d}{dt}(r\delta v_{\rm rot}) = 0, \tag{A2}$$

$$\frac{d}{dt}\delta v_T = -\frac{\partial v}{\partial r}\delta v_T, \tag{A3}$$

where $\delta v_T \equiv \delta v_r - \partial(r\delta v_\perp)/\partial r$ (see Lai & Goldreich 2000). The potential flow discussed in the main text corresponds to $\delta u = r\delta v_\perp$, $\delta v_T = 0$ and $\delta v_{\rm rot} = 0$. Note that $\delta v_{\rm rot}$ is decoupled from the potential flow.

Writing $\delta v_{\rm rot}$ in the self-similar form, $\delta v_{\rm rot}(r,t) = v_t(-t)^s\delta V_{\rm rot}(\eta)$, equation (A2) becomes

$$W(\eta\delta V_{\rm rot})' + (-s - 3 + 2\gamma)(\eta\delta V_{\rm rot}) = 0, \tag{A4}$$

where $W = V + (2 - \gamma)\eta$. Since $V \propto \eta$ as $\eta \to 0$, it is most natural to require $\delta V_{\rm rot} \propto \eta$ at $\eta \to 0$ (corresponding to a uniform "rotation"). Equation (A4) then gives $s = -1/3$, independent of γ. This is a growing mode which describes the spin-up of a rotating cloud during gravitational collapse (see Hanawa & Nakayama 1997; Matsumoto & Hanawa 1999). The "angular frequency" increases as $\delta v_{\rm rot}/r \propto (-t)^{-4/3}\delta V_{\rm rot}/\eta$, and the velocity perturbation increases as $\delta v_{\rm rot}/v \propto (-t)^{-1/3} \propto \rho_c(t)^{1/6}$.

Similarly, writing δv_T as $\delta v_T(r,t) = v_t(-t)^s\delta V_T(\eta)$, equation (A3) becomes

$$W\delta V_T' + (V' + \gamma - 1 - s)\delta V_T = 0. \tag{A5}$$

For $\eta \to 0$, we have $\delta V_r \propto \eta^{l-1}$, $\delta V_\perp \propto \eta^{l-1}$, but $\delta V_T \propto \eta^{l+1}$. Equation (A5) then gives $s = (4/3 - \gamma)l - 1/3$. This is the growing "votex" mode discussed by Hanawa & Matsumoto (2000b).

REFERENCES

Boily, C. M., & Lynden-Bell, D. 1995, MNRAS, 276, 133.

Bonnel, I. A. 1999, The Origin of Stars and Planetary Systems, ed. C. J. Lada & N. D. Kylafis (Kluwer Academic Pub.: Dordrecht).

Bonner, W. B. 1956, MNRAS, 116, 351.

Boss, A. P. 1998, ApJ, 501, L77.

Burkert, A., & Bodenheimer, P. 1996, MNRAS, 280, 1190.

Burkert, A., Bate, M. R., & Bodenheimer, P. 1997, MNRAS, 289, 497.

Burrows, A., Hayes, J., & Fryxell, B. A. 1995, ApJ, 450, 830.

Burrows, A., & Hayes, J. 1996, Phys. Rev. Lett., 76, 352.

Foster, P. N., & Chevalier, R. A. 1993, ApJ, 416, 303.

Galli, D., & Shu, F. H. 1993a, ApJ, 417, 220.

Galli, D., & Shu, F. H. 1993b, ApJ, 417, 243.

Goldreich, P., Lai, D., & Sahrling, M. 1996, in "Unsolved Problems in Astrophysics", ed. J. N. Bahcall and J. P. Ostriker (Princeton University Press).

Goldreich, P., & Weber, S. V. 1980, ApJ, 238, 990.

Goodman, A. A., Benson, P. J., Fuller, G. A., & Myers, P. C. 1993, ApJ, 406, 528.

Hanawa, T., & Nakayama, K. 1997, ApJ, 484, 238.

Hanawa, T., & Matsumoto, T. 1999, ApJ, 521, 703.

Hanawa, T., & Matsumoto, T. 2000a, PASJ, in press.

Hanawa, T., & Matsumoto, T. 2000b, astro-ph/0001447.

Herant, M., Benz, W., Hix, J., Colgate, S. A., & Fryer, C. 1994, ApJ, 395, 642.

Hunter, C. 1962, ApJ, 136, 594.

Hunter, C. 1977, ApJ, 218, 834.

Hunter, C. 1986, MNRAS, 223, 391.

Janka, H.-T. 1998, in Proc. of the 4th Ringberg Workshop on Neutrino Astrophysics (Munich, MPI).

Janka, H.-Th., & Müller, E. 1994, A&A, 290, 496.

Janka, H.-T., & Müller, E. 1996, A&A, 306, 167.

Lai, D. 1999, in *Stellar Astrophysics* (Proceedings of Pacific Rim Conference, Hong Kong, August, 1999), ed. K. S. Cheng (Kluwer Publication) (astro-ph/9912522).

Lai, D., & Goldreich, P. 2000, ApJ, 535, xxx (May 20) (astro-ph/9906400).

Larson, R. B. 1969, MNRAS, 145, 271.

Li, Z.-Y. 1998, ApJ, 493, 230.

Li, Z.-Y., & Shu, F. H. 1997, ApJ,

Lin, C. C., Mestel, L., & Shu, F. H. 1965, ApJ, 142, 1431.

Mathews, J., & Walker, R. L. 1970, Mathematical Methods of Physics (Addison-Wesley: New York).

Matsumoto, T., & Hanawa, T. 1999, ApJ, 521, 659.

Mouschovias, T. Ch., & Ciolek, G. E. 1999, in The Origin of Stars and Planetary Systems, ed. C. J. Lada & N. D. Kylafis (Kluwer Academic Pub.: Dordrecht).

Myhill, E. A., & Boss, A. P. 1993, ApJS, 89, 345.

Myers, P. C., Fuller, G. A., Goodman, A. A., & Benson, P. J. 1991, ApJ, 376, 561.

Penston, M. V. 1969, MNRAS, 144, 425.

Ori, A., & Piran, T. 1988, MNRAS, 234, 821.

Press, W. H., Teukolsky, S. A., Flannery, B. P., & Vetterling, W. T. 1992, Numerical Recipes (Cambridge University Press: Cambridge).

Safier, P. N., Mckee, C. F., & Stahler, S. W. 1997, ApJ, 485, 660.

Shu, F. H. 1977, ApJ, 214, 488.

Shu, F. H., Adams, F. C., & Lizano, S. 1987, ARA&A, 25, 23.

Shu, F. H., et al. 1999, in The Origin of Stars and Planetary Systems, ed. C. J. Lada & N. D. Kylafis (Kluwer Academic Pub.: Dordrecht).

Terebey, S., Shu, F. H., & Cassen, P. 1984, ApJ, 286, 529.

Truelove, J. K., Klein, R. I., McKee, C. F., et al. 1997, ApJ, 489, L179.

Truelove, J. K., Klein, R. I., McKee, C. F., et al. 1998, ApJ, 495, 821.

Unno, W., et al. 1989, Nonradial Oscillations of Stars (University of Tokyo Press).

Whitworth, A., & Summers, D. 1985, MNRAS, 214, 1.

Yahil, A. 1983, ApJ, 265, 1047.

Table 1.   Parameters for Pre-collapse Larson-Penston-Yahil Solutions

γ	D_0	η_s	$\mathcal{M}_\infty$
1.00	0.13256	2.34113	3.271
1.05	0.18299	2.33723	2.802
1.10	0.25908	2.33252	2.506
1.15	0.37769	2.32991	2.338
1.20	0.57228	2.33277	2.290
1.25	0.92455	2.34606	2.407
1.30	1.75375	2.38512	2.944
1.31	2.10358	2.40203	3.216
1.32	2.66174	2.42909	3.695
1.33	3.99500	2.49457	5.113

Note. — γ is the polytropic index, $D_0 = D(\eta = 0)$, η_s is the sonic point, where $W = A = (\gamma D^{\gamma-1})^{1/2}$, and $\mathcal{M}_\infty = (|V|/A)_\infty$ is the Mach number at $\eta \to \infty$.
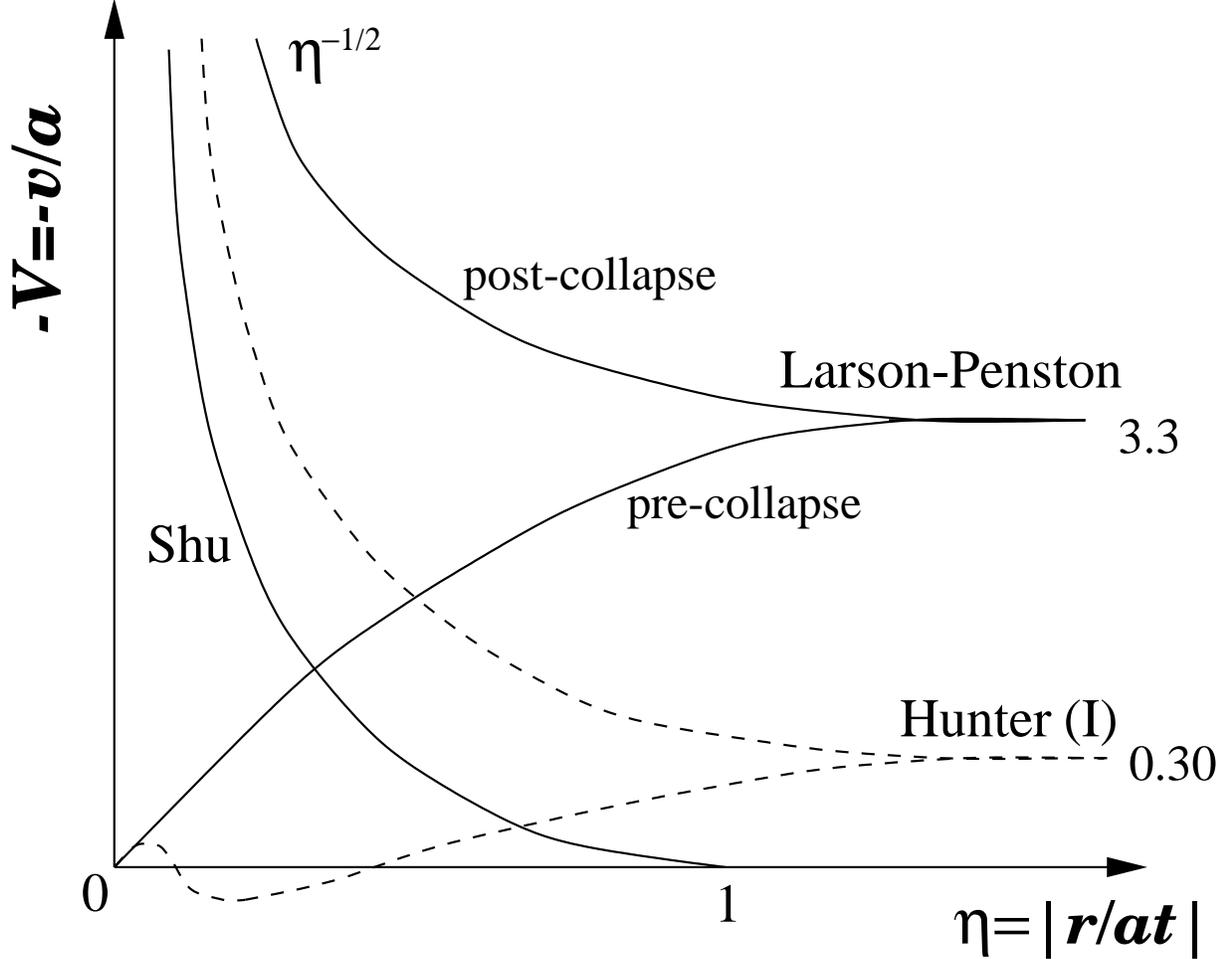
Fig. 1.— A schematic diagram showing the properties of different self-similar solutions describing the collapse and accretion of isothermal gas clouds. The similarity variable is $\eta = r/(-at)$ for pre-collapse solutions ($t < 0$) and $\eta = r/(at)$ for post-collapse (accretion) solutions ($t > 0$), where a is the sound speed, and $t = 0$ corresponds to the epoch when the central core collapses to form a protostar. The vertical axis gives the dimensionless inflow flow velocity $-V = -v/a$. Shu's expansion-wave solution (the solid curve that terminates at $\eta = 1$, the rarefaction wave front) describes post-collapse accretion, while the other solutions have a pre-collapse phase and a post-collapse phase which are connected at $\eta \to \infty$ (or $t = 0$). All post-collapse flows approach free-fall $V \propto \eta^{-1/2}$ as $\eta \to 0$. At $\eta \to \infty$, the Larson-Penston solution has Mach number of 3.3. The dashed curves give an examples of the infinite (but discrete) number of type I solutions found by Hunter (1977). (Note that the pre-collapse type I solutions contain regions with both positive and negative v.) The expansion-wave solution is the limiting case ($V \to 0$ at $\eta \to \infty$) of the post-collapse Type I solutions. Note that all pre-collapse solutions have $V \to -2\eta/3$ as $\eta \to 0$.
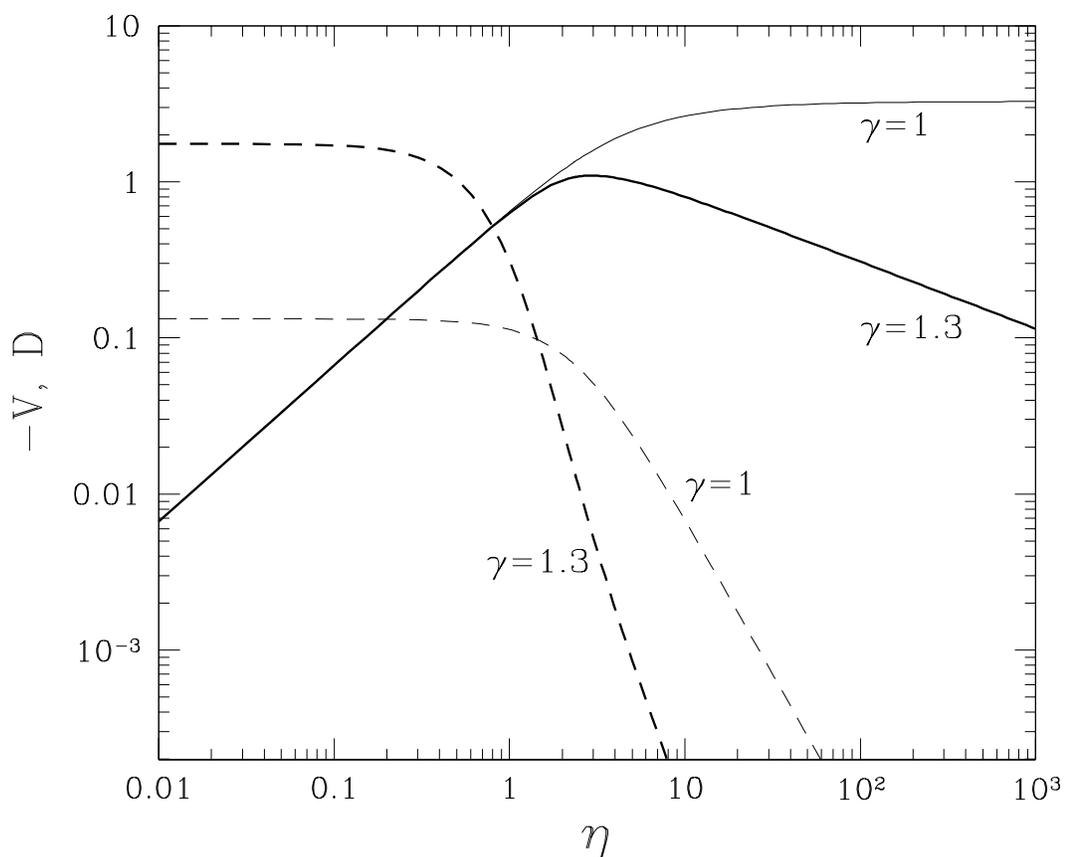
Fig. 2.— The Larson-Penston-Yahil similarity solutions are shown for $\gamma = 1$ and $\gamma = 1.3$. The solid curves give the dimensionless flow velocity $(-V)$, and the dashed curves give the density profile D.
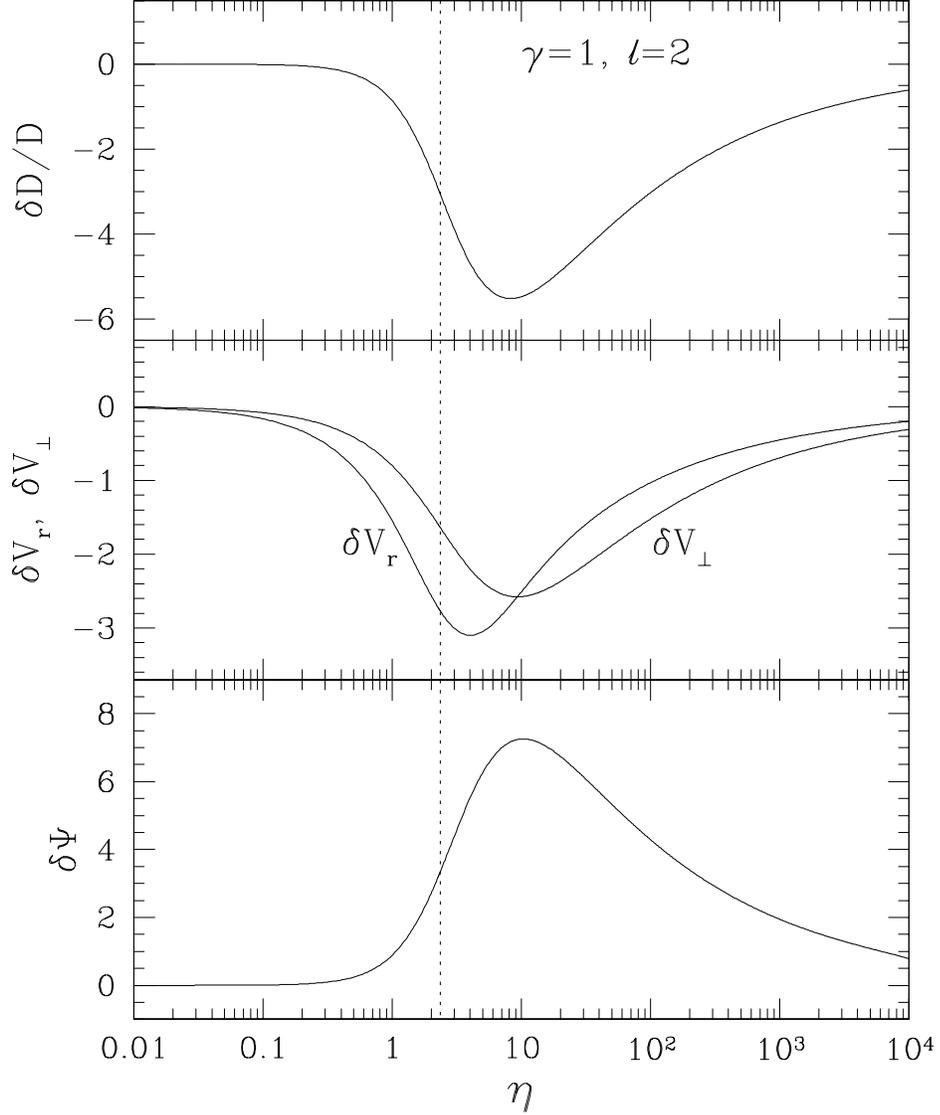
Fig. 3.— Eigenfunctions of the lowest-order bar-mode ($l = 2$) for $\gamma = 1$ (isothermal collapse), with the eigenvalue $s = -0.352$. The upper panel shows the fractional density perturbation $\delta D/D$, the middle panel shows the radial and tangential velocity perturbations, and the lower panel shows the potential perturbation. The dotted vertical line denotes the transonic point $\eta_s = 2.341$. The similarity variable is $\eta = r/(-at)$, where a is the (isothermal) sound speed.
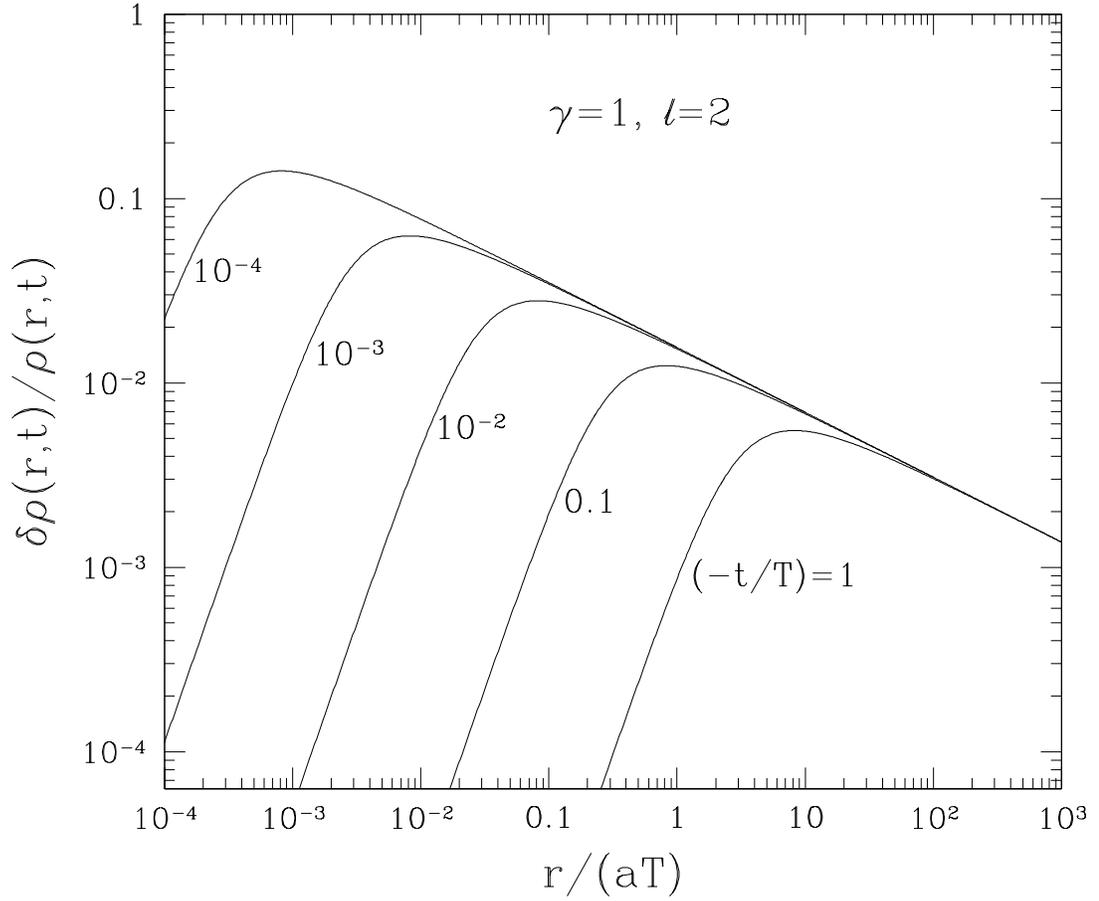
Fig. 4.— Evolution of the $l = 2$ density perturbation during the collapse of an isothermal cloud ($\gamma = 1$). The angular dependence, Y_{2m}, has be suppressed. Note that $\delta\rho(r,t)/\rho(r,t) \propto (-t)^{-0.352}\delta D(\eta)/D(\eta)$, with $\eta = r/(-at)$; T is a fiducial time, and a is the sound speed. The different curves correspond to different times. The center of the cloud reaches singularity as t approaches zero.
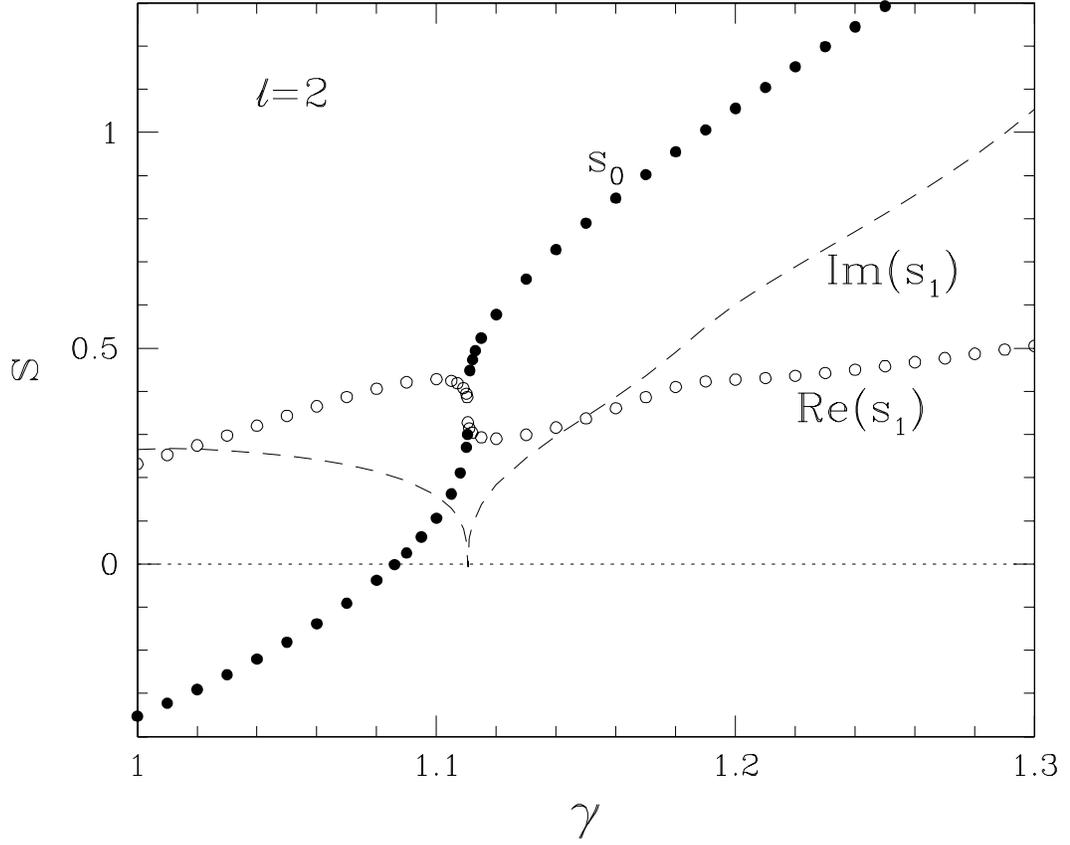
Fig. 5.— The eigenvalue s of the bar-mode ($l = 2$) as a function of the polytropic index γ. The filled circles correspond to the lowest-order mode (with no radial node in the eigenfunction), with $s = s_0$ real; The open circles correspond to $\mathrm{Re}(s_1)$ of a higher-order mode, with $s = s_1$ complex, the dashed curve gives $\mathrm{Im}(s_1)$ of the same mode. Note that the lowest-order bar mode is globally unstable for $\gamma \leq 1.09$. The $s = s_1$ mode has one radial node for $\gamma \leq 1.15$, and it crosses the zero-node mode ($s = s_0$) at $\gamma \simeq 1.11$. For $\gamma \geq 1.11$, the $s = s_1$ mode is the mode with the lowest $\mathrm{Re}(s_1)$.
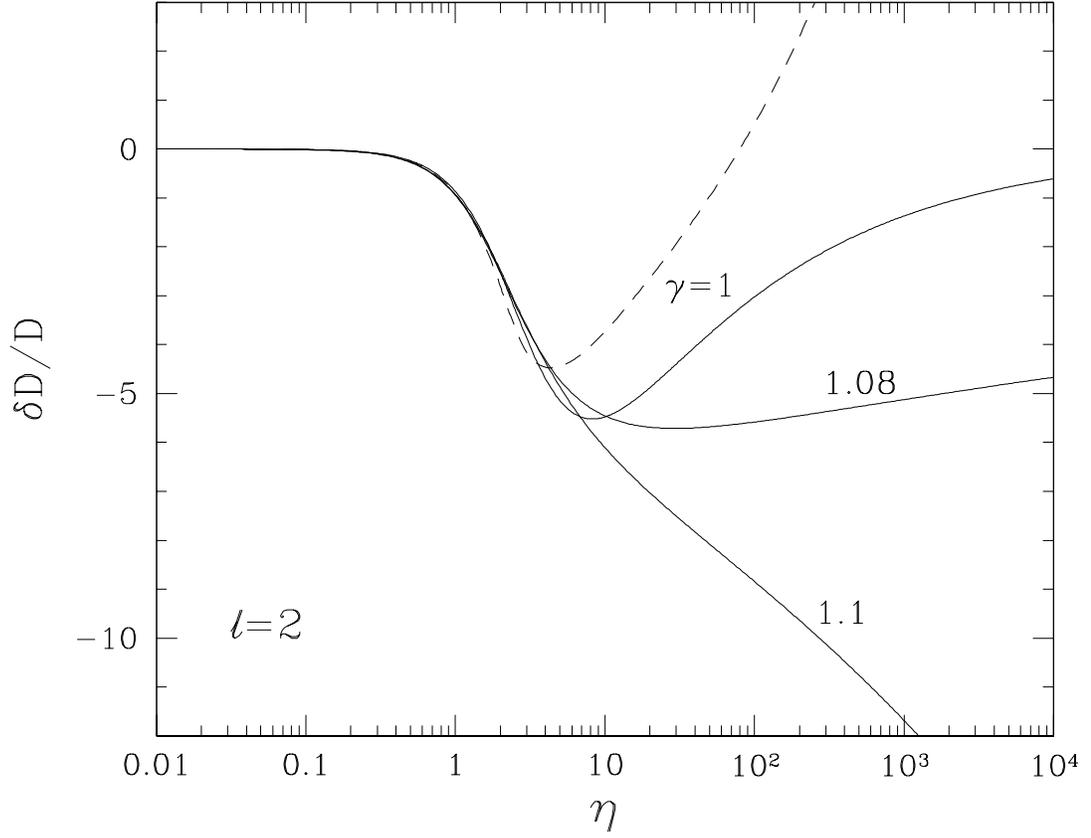
Fig. 6.— The eigenfunctions $\delta D/D$ of several bar-modes ($l = 2$) for different γ. The solid curves correspond to the lowest-order bar-mode for $\gamma = 1$ (with $s = -0.352$, unstable), $\gamma = 1.08$ (with $s = -0.038$, unstable), and $\gamma = 1.1$ (with $s = 0.106$, stable). The dashed curve gives $\mathrm{Re}(\delta D/D)$ for the $s = s_1 = 0.23 + 0.26i$ mode (see Fig. 5) with $\gamma = 1$.
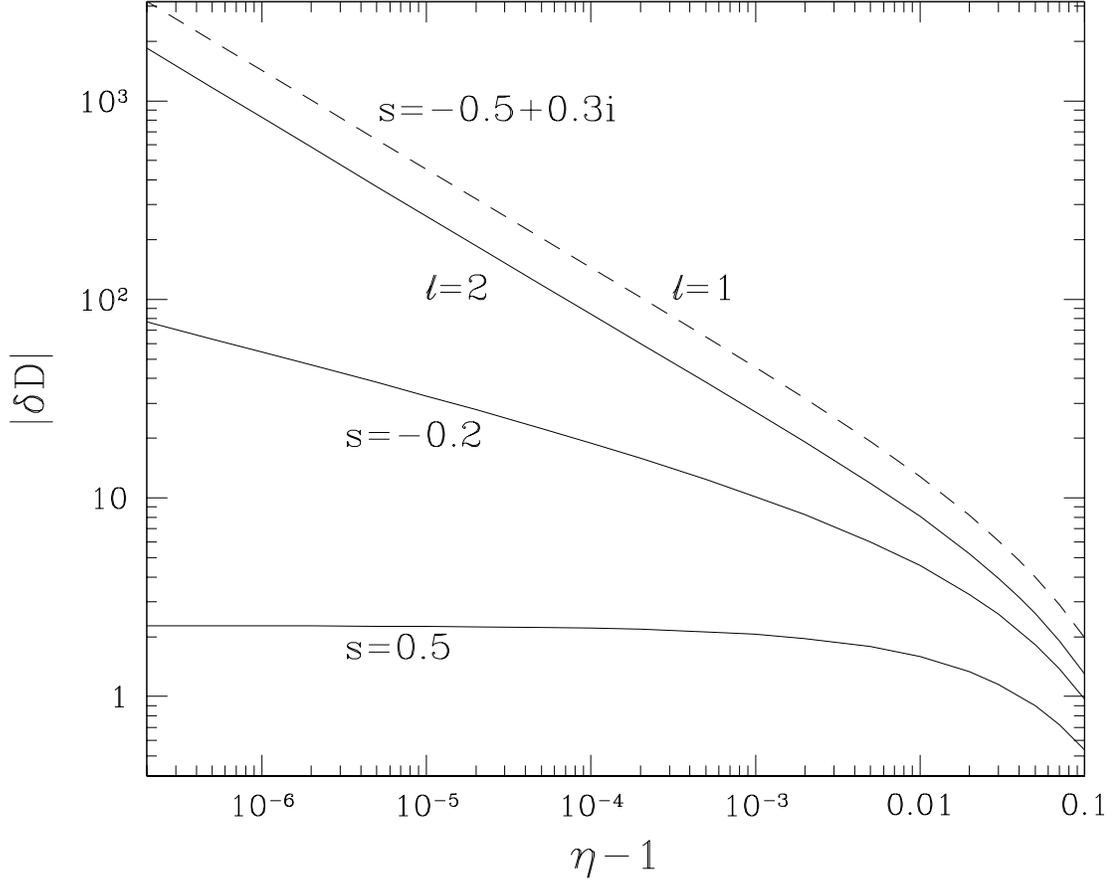
Fig. 7.— Behavior of the absolute value of the density perturbation δD just outside the expansion-wave front ($\eta = 1$) in the expansion-wave solution. The solid curves are for $l = 2$ and the dashed curve for $l = 1$. The values of s are labeled for each curve. Note that when $\mathrm{Re}(s) < 0$, the perturbation $|\delta D| \to \infty$ as $\eta \to 1$.